

# The 1976 Helios and Pioneer Solar Conjunctions— Continuing Corroboration of the Link Between Doppler Noise and Integrated Signal Path Electron Density

A. L. Berman, J. A. Wackley, and S.T. Rockwell  
DSN Network Operations Section

*Observed doppler noise (rms phase jitter) from the 1976 solar conjunctions of the Helios 1 and 2 and the Pioneer 10 and 11 spacecraft was processed with a recently developed doppler noise model “ISEDB.” Good agreement is obtained between the observed data and the model. Correlation is shown between deviations from the ISEDB model and sunspot activity, but it is insufficient to be modeled. Correlation is also shown between ISEDB model deviations for (spacecraft) signal paths on the same side of the sun.*

## I. Introduction

Utilizing observed doppler noise data from the 1975 Helios 1, Pioneer 10 and Pioneer 11 Solar Conjunctions, the authors have constructed a geometric model (the “ISED” series) for plasma-induced doppler noise (rms phase jitter). The functional form of the model was developed by assuming that doppler noise was proportional to the integrated signal path electron density, with the electron density assumed to be:

$$N_e(r) = \frac{A}{r^6} + \frac{B}{r^{2.3}}$$

*r* = heliocentric distance

Reference 1 describes a modification to the model (“ISEDB”) which accounts for heliocentric latitude; Refs. 2 through 5 document the development of the basic model. The most recent model—ISEDB—is defined as follows:

ISEDB =

$$\left[ \left( \left\{ A_0 \left[ \frac{\beta}{(\sin \alpha)^{1.3}} \right] F(\alpha, \beta) + A_1 \left[ \frac{1}{(\sin \alpha)^5} \right] \right\} 10^{-A_s(\phi_s/90)} \right)^2 + (0.0015)^2 \right]^{1/2}$$

where

$$F(\alpha, \beta) = 1 - 0.05 \left\{ \frac{(\beta - \pi/2 + \alpha)^3 - (\alpha - \pi/2)^3}{\beta} \right\} \\ - 0.00275 \left\{ \frac{(\beta - \pi/2 + \alpha)^5 - (\alpha - \pi/2)^5}{\beta} \right\}$$

$\alpha$  = Sun-Earth-Probe angle (SEP), rad

$\beta$  = Earth-Sun-Probe angle (ESP), rad

and

$\phi_s$  = heliographic latitude, deg

$$= \sin^{-1} [\cot \alpha (-\cos \delta_d \sin \alpha_{ra} \sin \epsilon + \sin \delta_d \cos \epsilon)]$$

$\alpha_{ra}$  = right ascension

$\delta_d$  = declination

$\epsilon$  = the obliquity of the ecliptic (23.445 deg)

with

$$A_0 = 9.65 \times 10^{-4}$$

$$A_1 = 5 \times 10^{-10}$$

$$A_8 = 9 \times 10^{-1}$$

It will be the intent of this article to ascertain if the Helios 1 and 2 and the Pioneer 10 and 11 observed doppler noise continues to be well represented by the ISEDB model.

## II. Data Description

The data consists of pass average, good, two-way doppler noise collected during the following time intervals (DOY = Day of Year, 1976):

Spacecraft	Begin (DOY)	End (DOY)
Pioneer 10	51	175
Pioneer 11	79	215
Helios 1	75	293
Helios 2	90	293

All doppler data was taken at a 60-sec sample rate with the exception of some Helios 2 passes, which utilized

doppler sample rates of either 10 or 1 second. In these cases, the following relationship was used to transform the doppler noise from the actual sample rate to an "equivalent" 60-s sample rate:

$$\text{noise}_{SR1} = \text{noise}_{SR2} \left( \frac{SR2}{SR1} \right)^{0.285}$$

where

$$SR1,2 = \text{sample rate } 1, 2$$

The collected noise data was fit with the ISEDB model and a new  $A_0$  was selected to minimize the standard deviation of the residuals:

$$A_0 = 11.21 \times 10^{-4}$$

Scatter diagrams for the data (observed doppler noise vs the ISEDB model) are seen as follows:

Fig. 1—Pioneer 10

Fig. 2—Helios 1

Fig. 3—Helios 2

Fig. 4—Combined

while the following figures present observed doppler noise and the ISEDB model as a function of DOY:

Fig. 5—Pioneer 10

Fig. 6—Pioneer 11

Fig. 7—Helios 1

Fig. 8—Helios 2

Examination of these figures leads one to conclude in a qualitative sense that the (ISEDB) model continues to be in good agreement with the doppler noise observations during the 1976 Pioneer 10 and 11 and Helios 1 and 2 solar conjunctions. The statistics of the observed doppler noise as fit to the ISEDB model were as follows, with "dB" =  $10 \log_{10} (\text{observed noise}/\text{ISEDB})$ :

	Pioneer 10	Pioneer 11	Helios 1	Helios 2	All
$\sigma, \text{dB}$	2.04	1.77	2.47	2.65	2.28
Bias, dB	-0.37	-0.01	-0.63	+1.36	+0.02

### III. Correlation of Observed Doppler Noise With Sunspot Activity

In Ref. 2, the authors attempted to correlate observed doppler noise with sunspot activity (the "RISED" model). Although a quantitative correlation with sunspot activity (as measured by  $R_z$  = Zurich (daily) sunspot index) was demonstrated, it was not (at that time) considered optimistically. The data presented in this report was processed with the RISED model (now "RISEDB"), and a new  $A_0$  to minimize the standard deviation was computed to be

$$A_0 = 10.16 \times 10^{-4}$$

Basically, the RISEDB performance (as compared to the ISEDB modeling) can be summarized by spacecraft as follows:

- Pioneer 10—significant degradation
- Pioneer 11—minor improvement
- Helios 1 —significant improvement
- Helios 2 —unchanged
- All —minor improvement

The statistics are as follows:

	Pioneer 10	Pioneer 11	Helios 1	Helios 2	All
$\sigma$ , dB	2.25	1.72	2.20	2.65	2.22
Bias, dB	-0.43	+0.30	-0.53	+1.06	+0.05

ISEDB residuals, "smoothed/phased" sunspots ( $\equiv XR_2$ ; see Ref. 2), and RISEDB residuals are seen in the following figures:

Fig. 9 —Pioneer 11

Fig. 10—Helios 1

Fig. 11—Helios 2

Regions which appear to show evidence of correlation between observed doppler noise and sunspot activity are as follows:

Pioneer 11, DOY 80–145 (Fig. 9)

Helios 1, DOY 75–175 (Fig. 10)

Helios 2, DOY 90–135 (Fig. 11)

However, these regions must be balanced against regions of little or even negative correlation, as follows:

Pioneer 11, DOY 175–195 (Fig. 9)

Helios 1, DOY 185–255 (Fig. 10)

Helios 2, DOY 140–170 (Fig. 11)

### IV. Multispacecraft Correlation

One would expect to see good correlation between ISEDB residuals from different spacecraft, as long as the signal paths are on the same side of the sun. Figure 12 shows ISEDB residuals for Pioneer 10, Pioneer 11, and Helios 2 when these signal paths were east (left) of the sun, while Fig. 13 shows ISEDB residuals for Pioneer 10, Pioneer 11, Helios 1, and Helios 2 when these signal paths were west (right) of the sun. Regions of correlation between various spacecraft are as follows:

HE 1/HE 2, DOY 90–134 (Fig. 13)

PN 11/HE 1, DOY 180–215 (Fig. 13)

PN 10/PN 11, DOY 80–105 (Fig. 12)

### V. Summary

Observed doppler noise data from the 1976 solar conjunction phases of the Pioneer 10 and 11 and the Helios 1 and 2 spacecraft was fit to the ISED model ("ISEDB") and subsequently shown to be in good agreement with the model—thus continuing to corroborate the direct link between observed doppler noise and integrated signal path electron density. Some evidence of correlation between sunspot activity and doppler noise is seen (the RISED model), but the relationship is insufficient to model in a quantitative fashion. Finally, correlation between doppler noise deviations from the ISEDB model continue to be seen for (spacecraft) signal paths on the same side of the sun.

## Acknowledgments

The authors would like to thank C. Darling and M. F. Cates, who rendered the illustrations, and J. DeNino, who typed this article.

## References

1. Berman, A. L., Wackley, J. A., Rockwell, S. T., and Yee, J. G., "The Pioneer 11 1976 Solar Conjunction: A Unique Opportunity to Explore the Heliographic Latitudinal Variations of the Solar Corona," in *The Deep Space Network Progress Report 42-35*, Jet Propulsion Laboratory, Pasadena, Calif., Oct. 15, 1976.
2. Berman, A. L., and Wackley, J. A., "Doppler Noise Considered as a Function of the Signal Path Integration of Electron Density," in *The Deep Space Network Progress Report 42-33*, Jet Propulsion Laboratory, Pasadena, Calif., June 15, 1976.
3. Berman, A. L., "Analysis of Solar Effects Upon Observed Doppler Data Noise During the Helios 1 Second Solar Conjunction," in *The Deep Space Network Progress Report 42-32*, Jet Propulsion Laboratory, Pasadena, Calif., April 15, 1976.
4. Berman, A. L., and Rockwell, S. T., "Correlation of Doppler Noise During Solar Conjunctions with Fluctuations in Solar Activity," in *The Deep Space Network Progress Report 42-30*, Jet Propulsion Laboratory, Pasadena, Calif., Dec. 15, 1975.
5. Berman, A. L., and Rockwell, S. T., "Analysis and Prediction of Doppler Noise During Solar Conjunctions," in *The Deep Space Network Progress Report 42-30*, Jet Propulsion Laboratory, Pasadena, Calif., Dec. 15, 1975.
6. Berman, A. L., "Solar Plasma Induced Doppler Noise Dependence Upon Sample Rate," IOM 421G-76-155, July 13, 1976 (a JPL internal document).

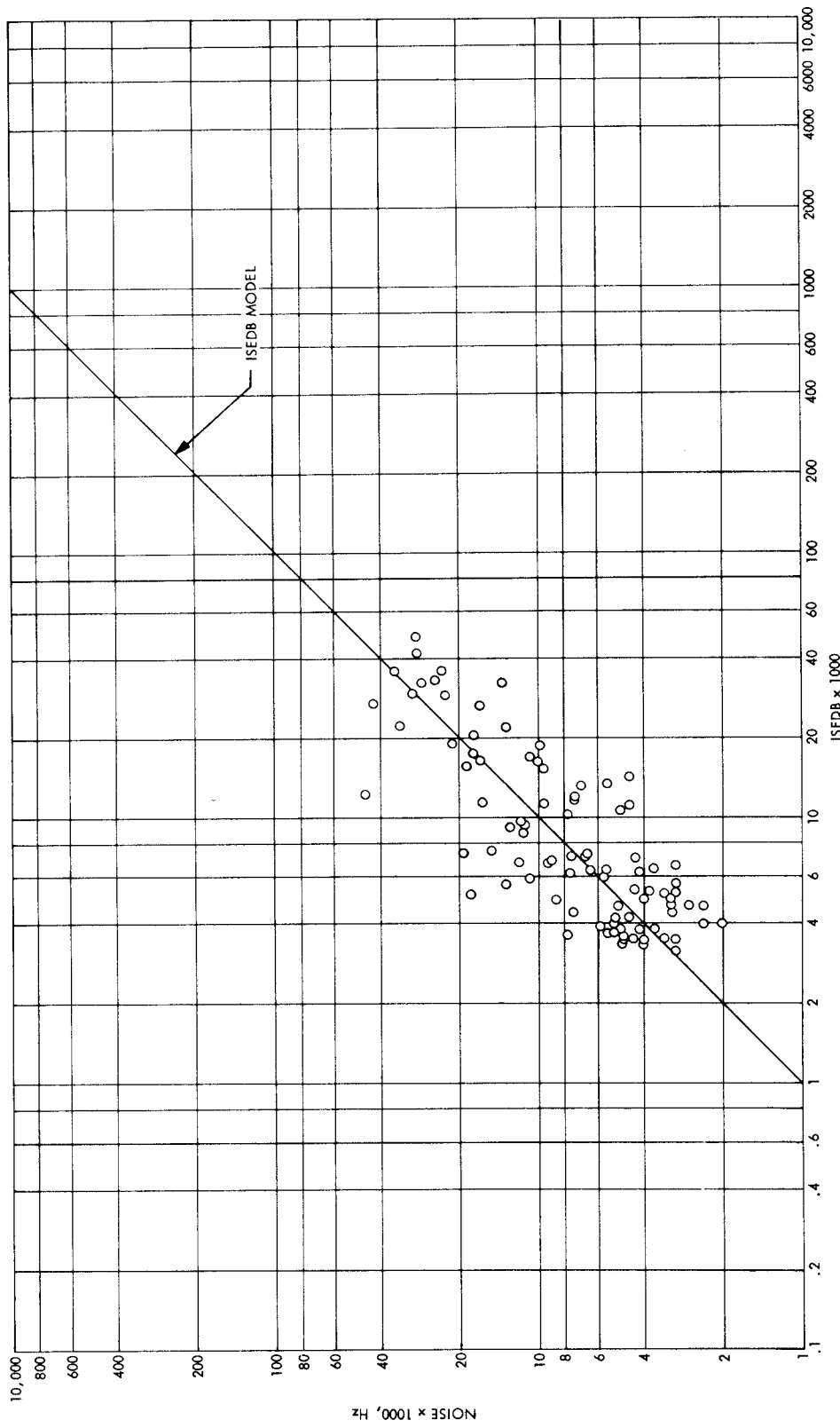


Fig. 1. Pioneer 10 (S/C 23) 1976 solar conjunction, observed doppler noise vs the ISEDDB model

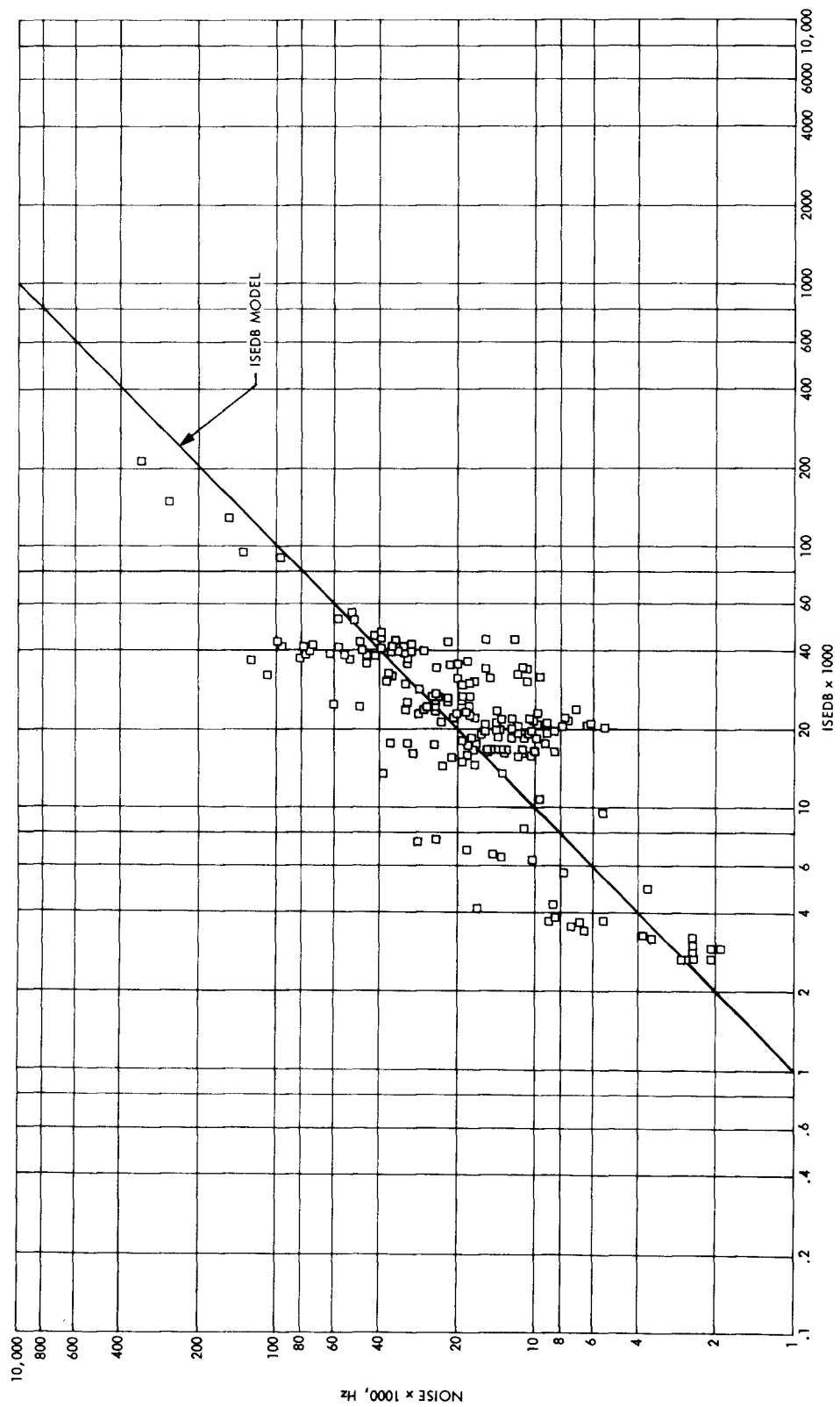


Fig. 2. Helios 1 (S/C 90) 1976 solar conjunction, observed doppler noise vs the ISEDDB model

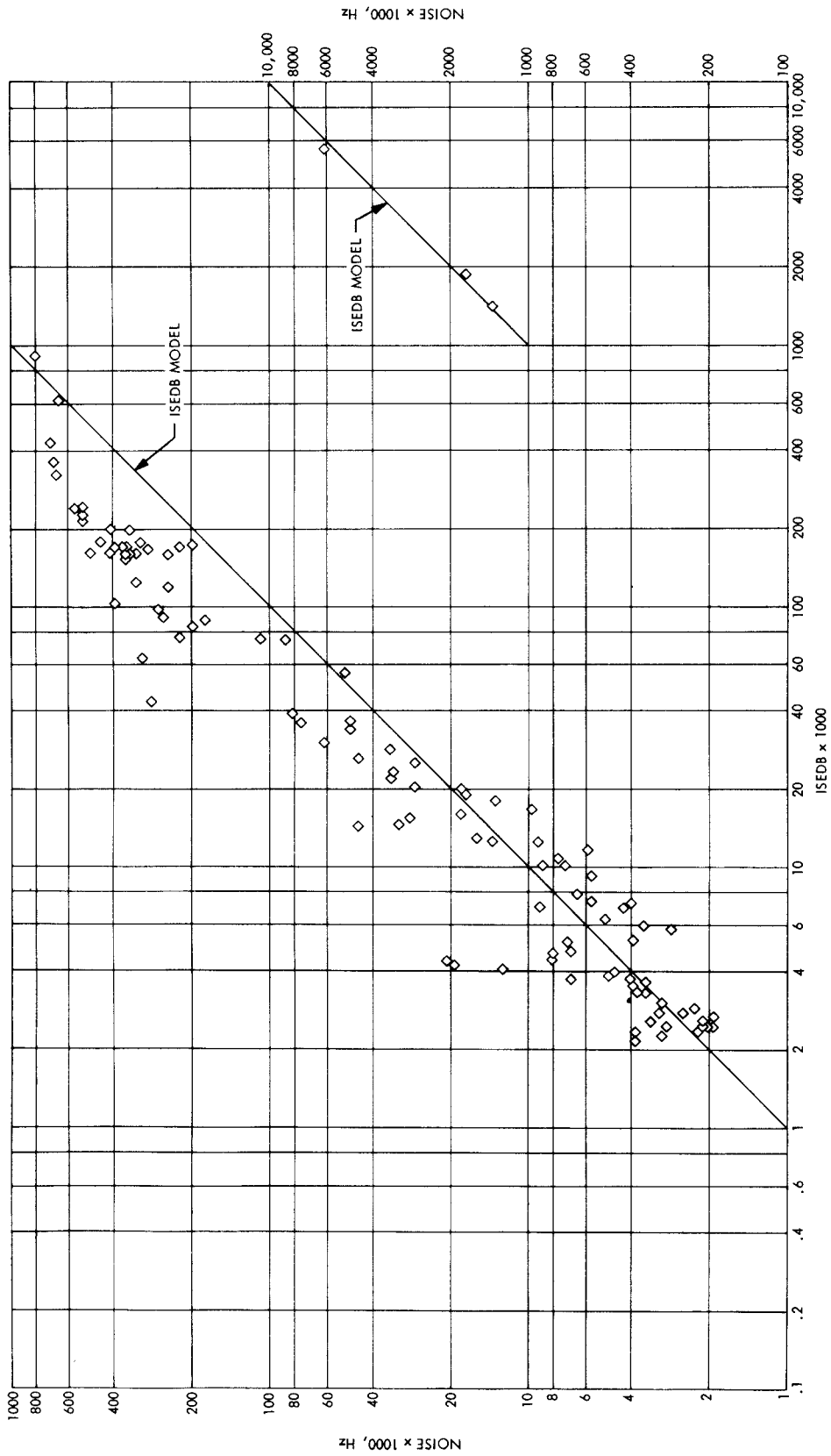


Fig. 3. Helios 2 (S/C 91) 1976 solar conjunction, observed doppler noise vs the ISEDDB model

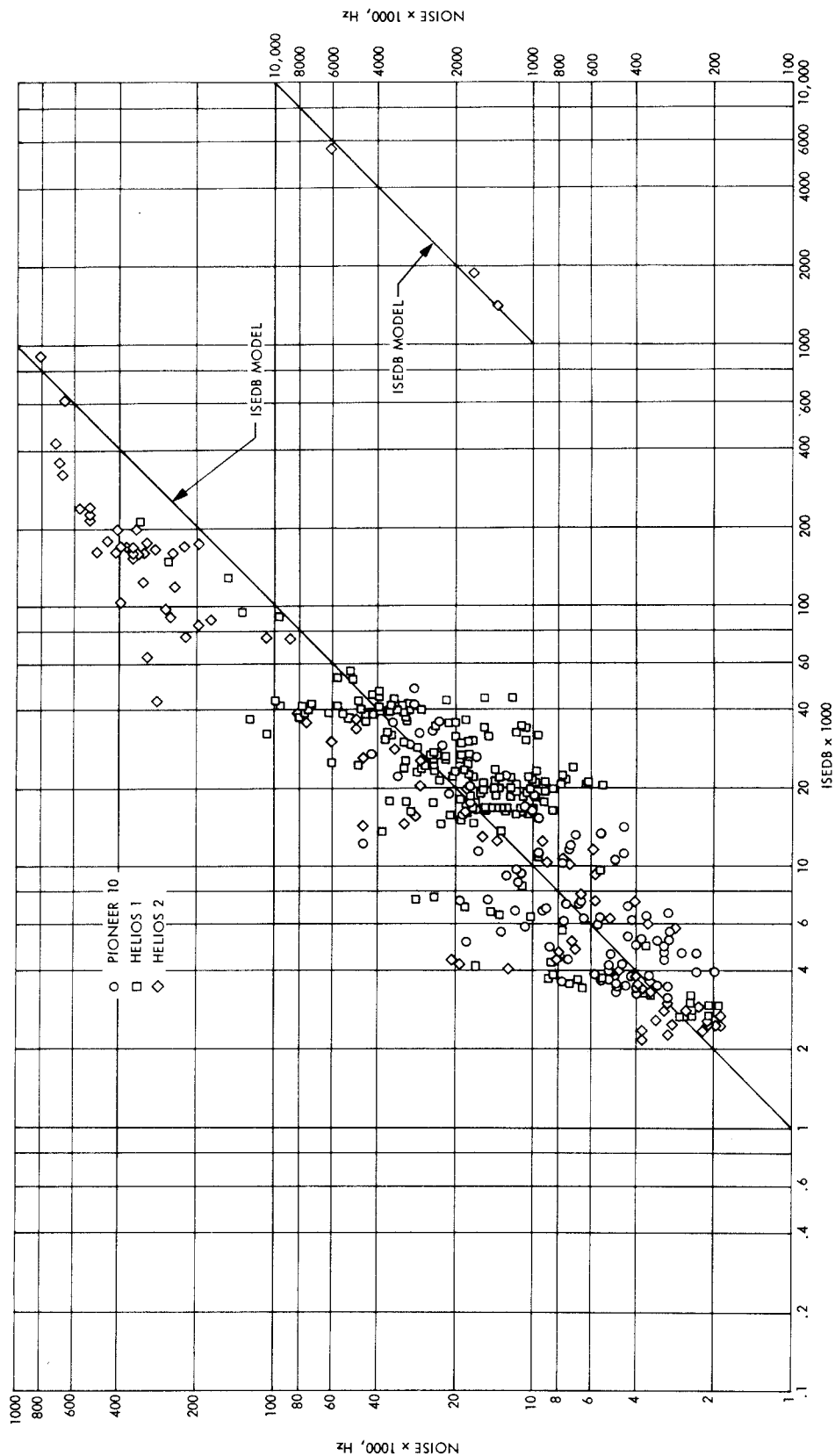


Fig. 4. Early 1976 solar conjunction mission composite, observed doppler noise vs the ISED8 model

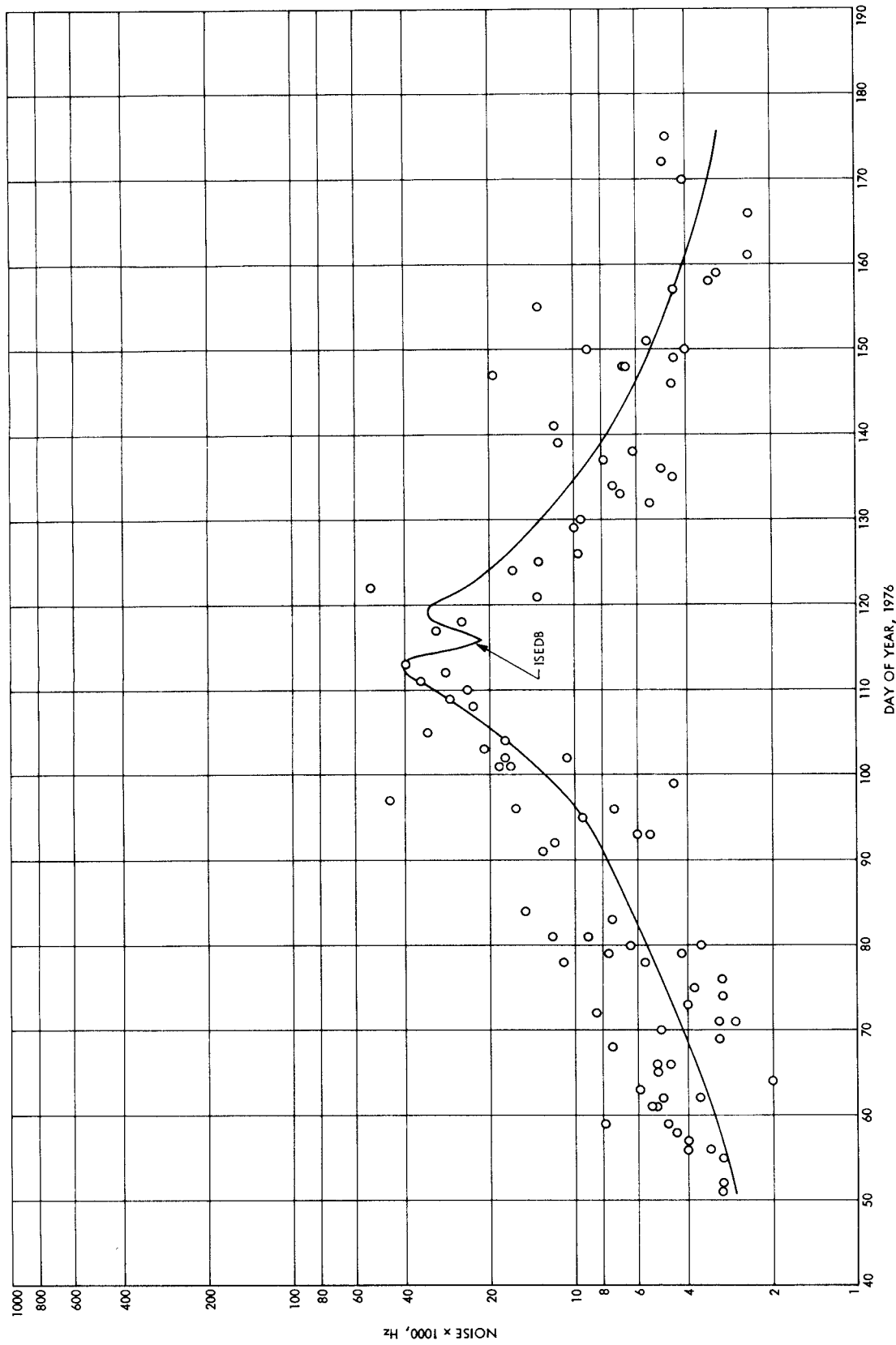


Fig. 5. Pioneer 10 1976 solar conjunction, observed doppler noise and the ISEDDB model vs day of year

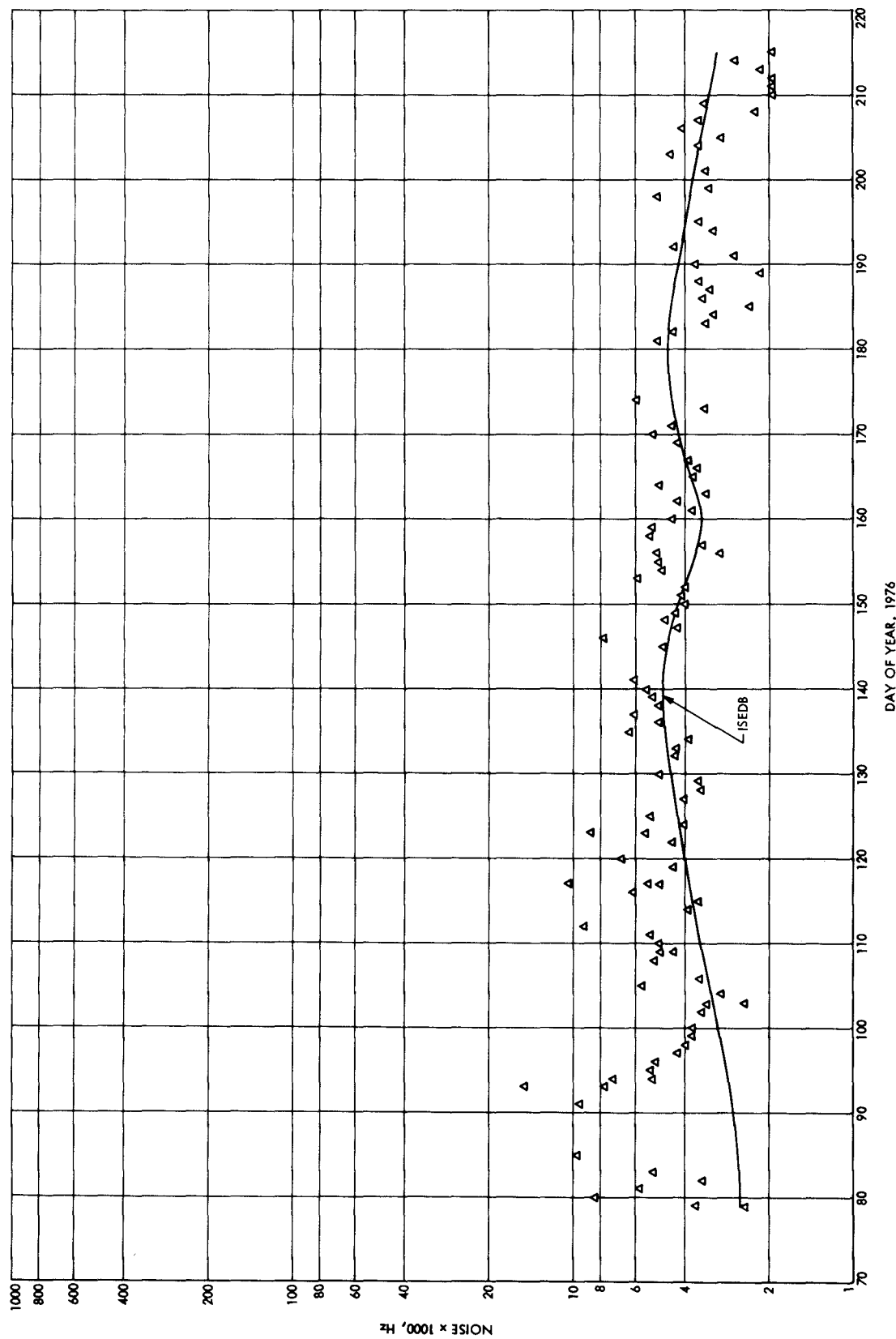


Fig. 6. Pioneer 11 1976 solar conjunction, observed doppler noise and the ISEDB model vs day of year

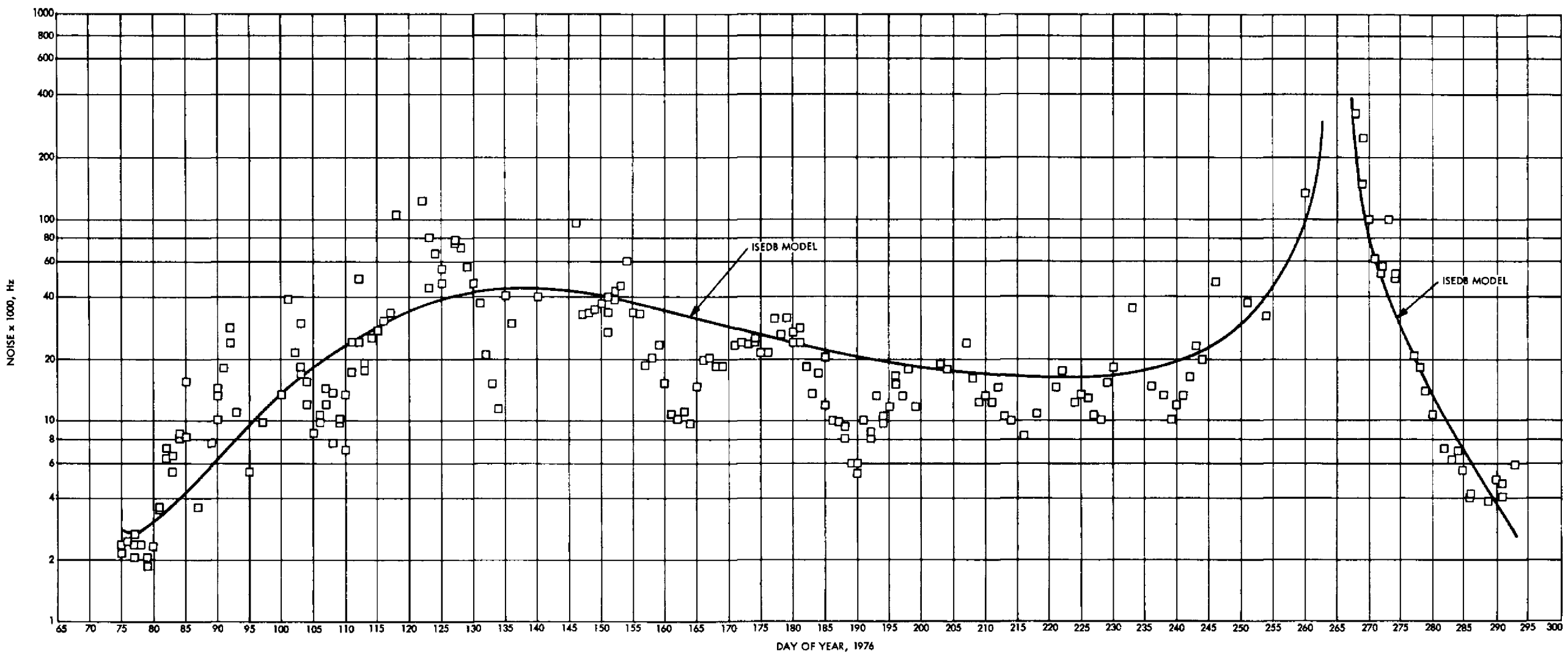


Fig. 7. Helios 1 1976 solar conjunction, observed doppler noise and the ISEDDB model vs day of year

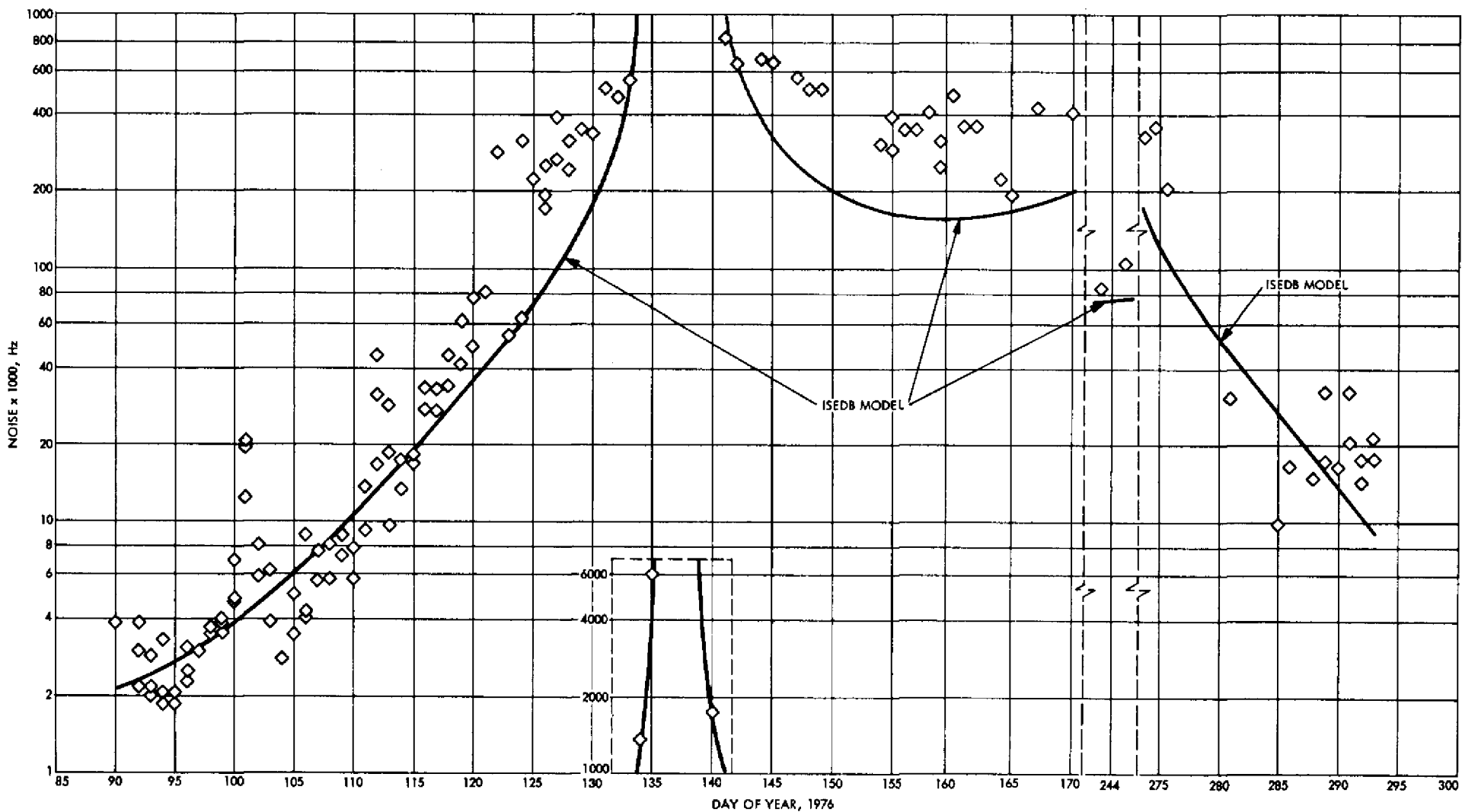


Fig. 8. Helios 2 1976 solar conjunction, observed doppler noise and the ISEDDB model vs day of year

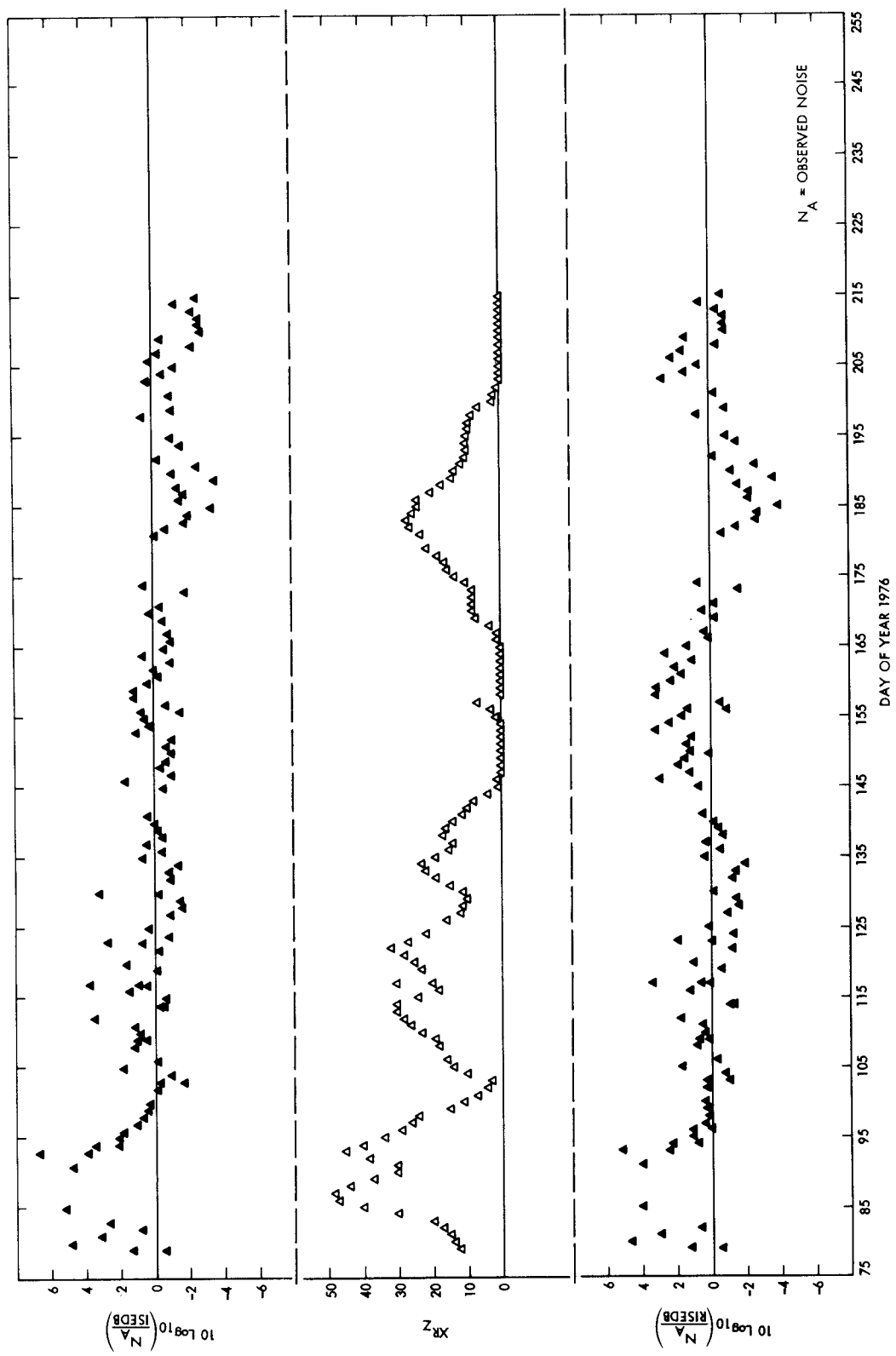


Fig. 9. Pioneer 11 1976 solar conjunction, ISEDZ residuals, RISEDB residuals and (smoothed/phased) sunspots vs day of year

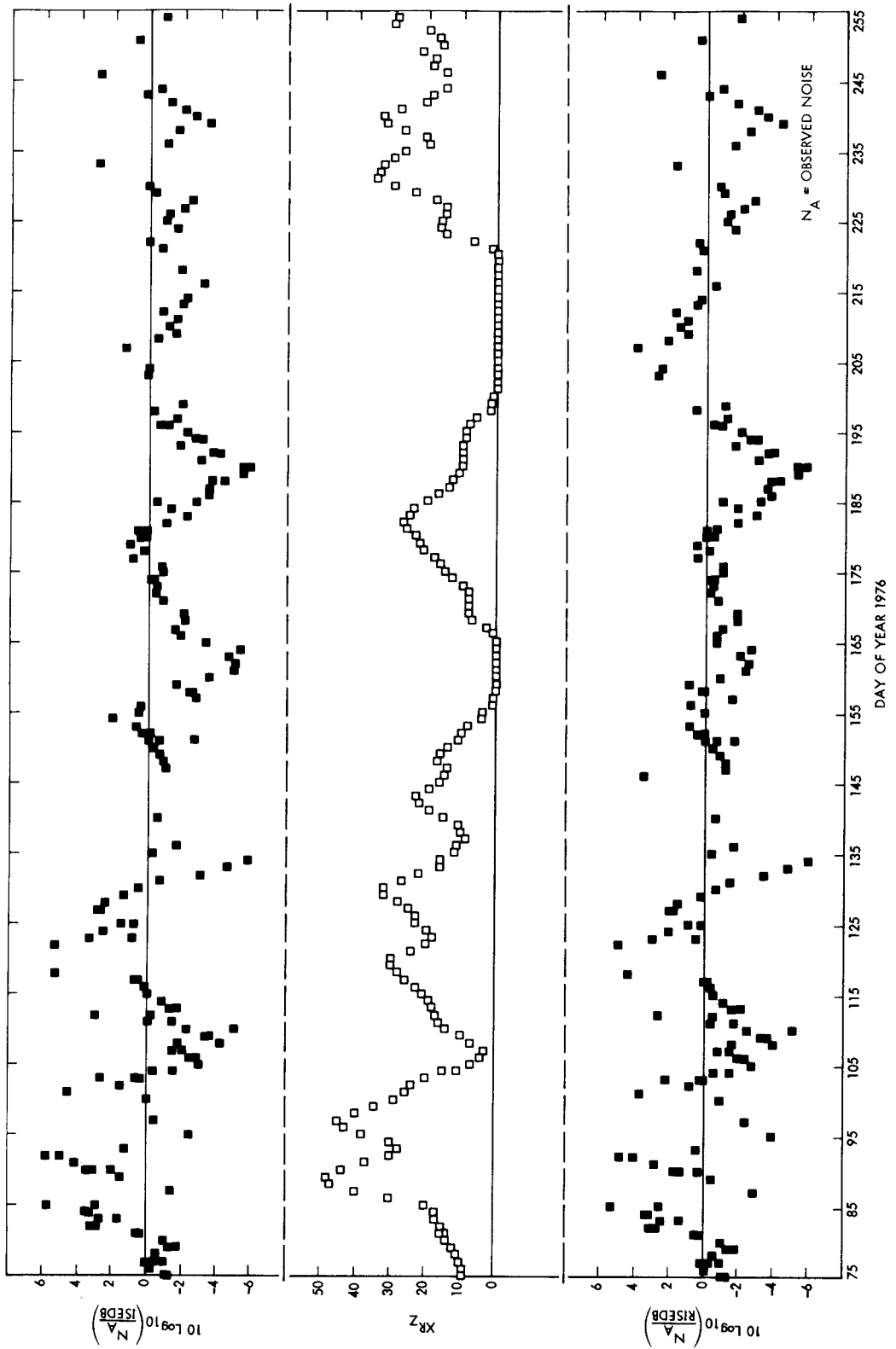


Fig. 10. Helios 1 1976 solar conjunction, ISED8 residuals, RISEDB residuals and (smoothed/phased) sunspots vs day of year

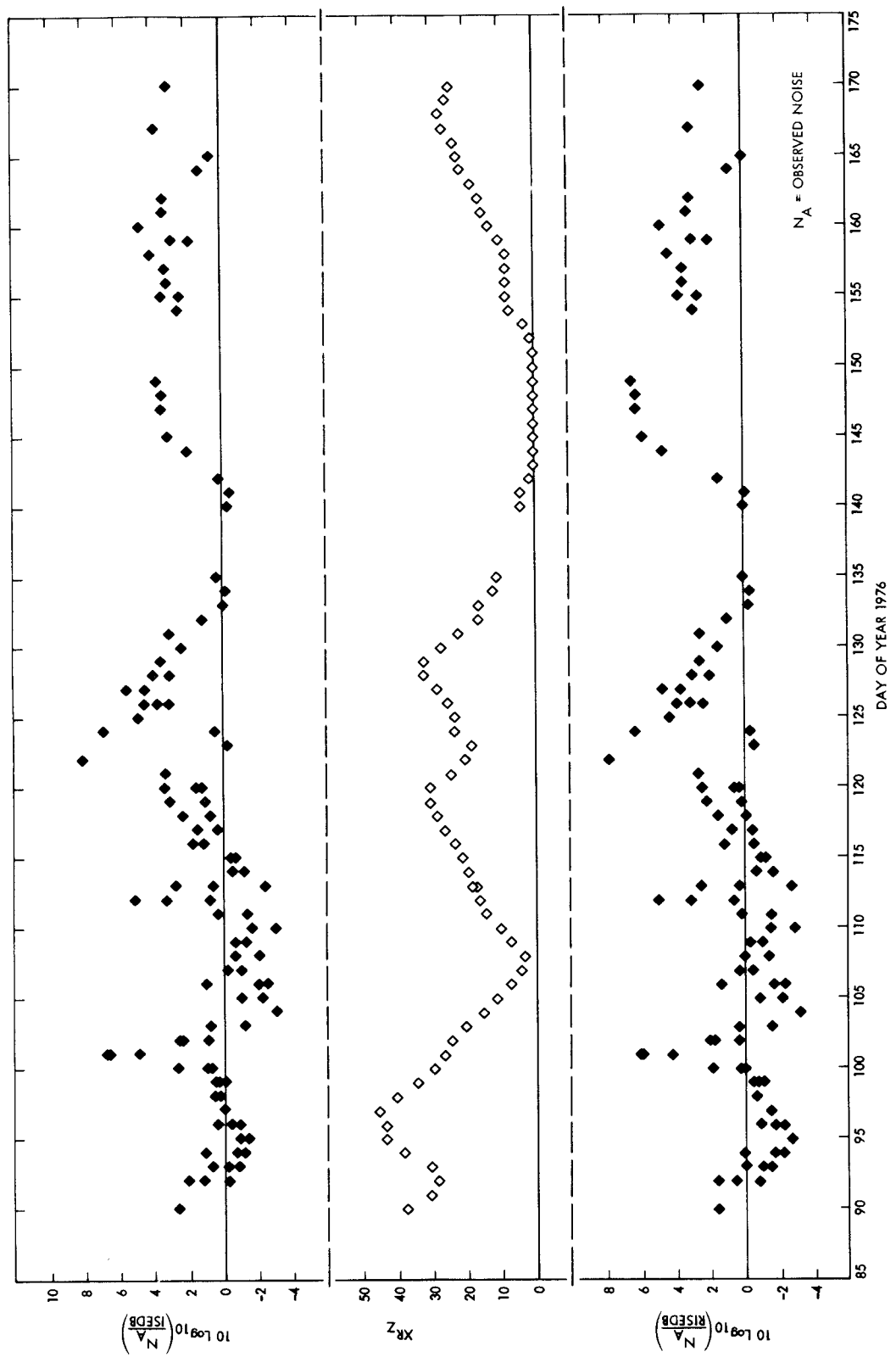
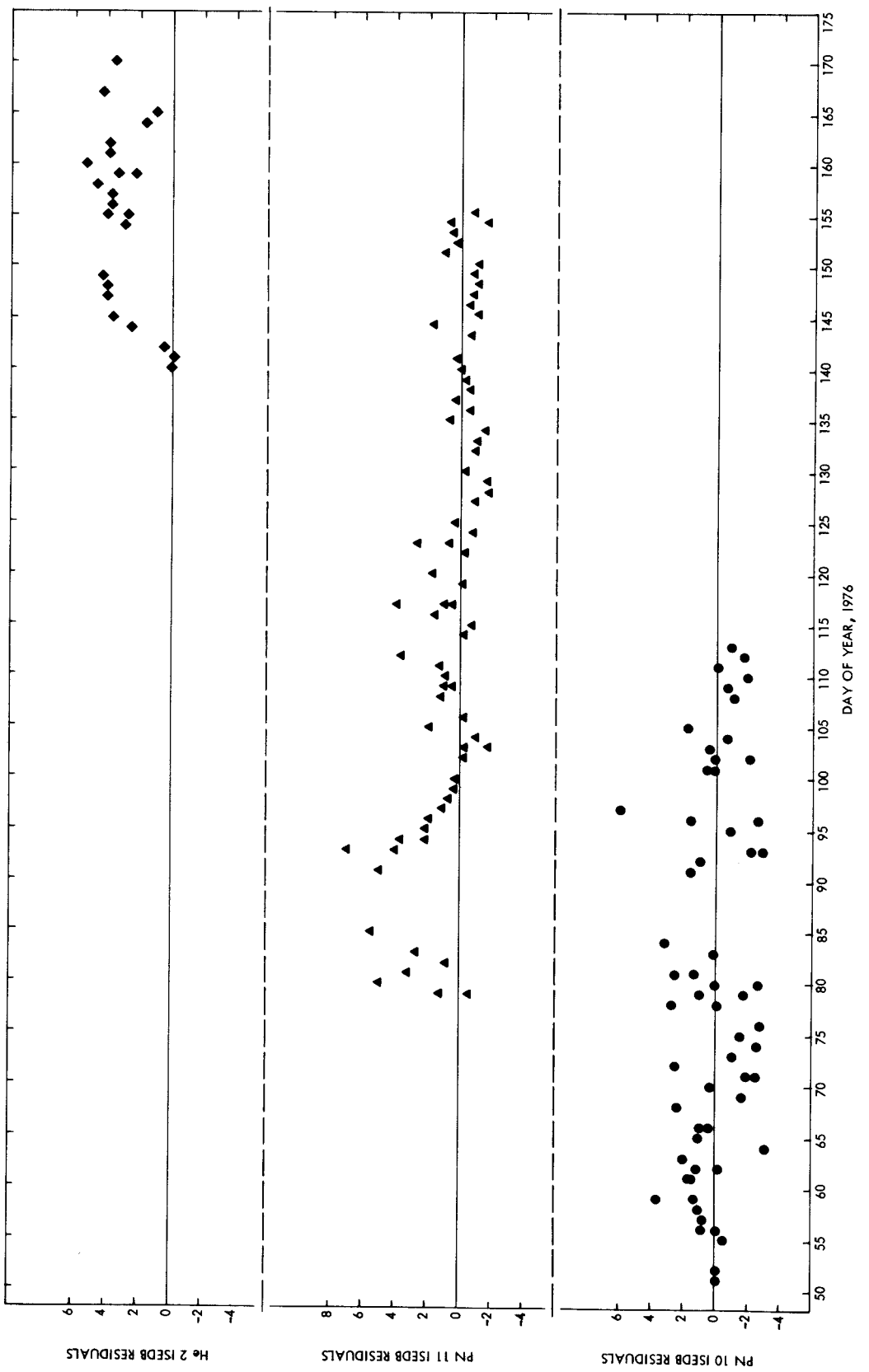


Fig. 11. Helios 2 1976 solar conjunction, ISEDB residuals, RISEDB residuals and (smoothed/phased) sunspots vs day of year



**Fig. 12. Multispacecraft ISED8 residual comparisons for signal paths east of the sun**

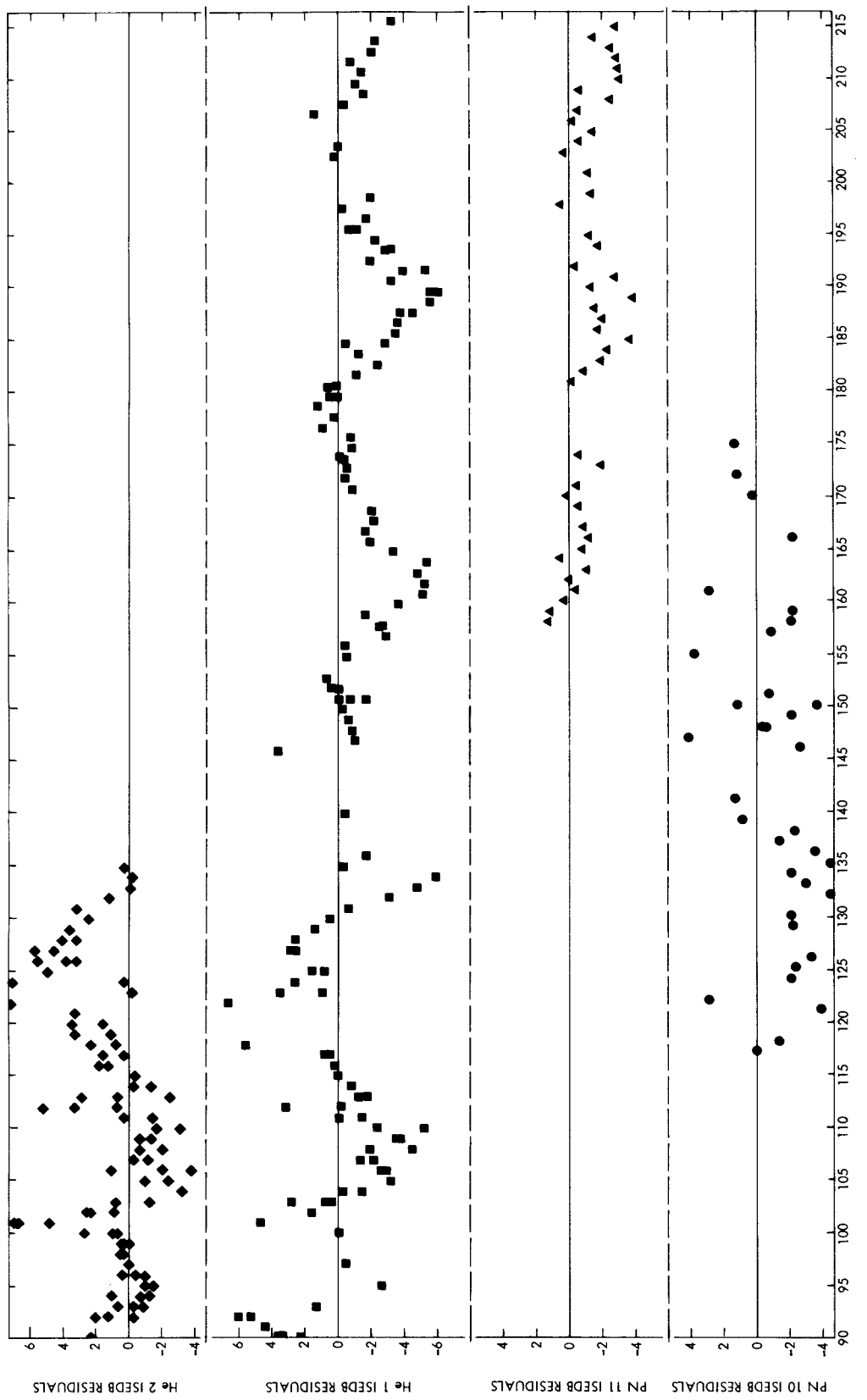


Fig. 13. Multispacecraft ISEDDB residual comparisons for signal paths west of the sun